Supplementary Materials for

A Jurassic ornithischian dinosaur from Siberia with both feathers and scales

Pascal Godefroit,* Sofia M. Sinitsa, Danielle Dhouailly, Yuri L. Bolotsky, Alexander V. Sizov, Maria E. McNamara, Michael J. Benton, Paul Spagna

*Corresponding author. E-mail: pascal.godefroit@naturalsciences.be

This PDF file includes:

Materials and Methods
Supplementary Text
Figs. S1 to S11
References (*29–55*)

Materials and Methods

This published work and the nomenclatural acts it contains have been registered in ZooBank, the proposed online registration system for the International Code of Zoological Nomenclature. The ZooBank life science identifiers can be resolved and the associated information viewed by appending the life science identifiers to the prefix http://zoobank.org/. The life science identifiers for this publication are urn:lsid:zoobank.org:pub:A7CCA9E4-2B87-43D9-A8CD-6D80C5165670, urn:lsid:zoobank.org:act: D479B27D-1F7F-4943-8DB1-F099E37101AA, and urn:lsid:zoobank.org:act:343881D7-FC69-4117-891F-CB0D411D25FF.

Supplementary Text

Geological Setting

The Kulinda locality is located in the Chernyshevsky District of the Chita Region (Zabaikalsky Krai), about 220 km to the east of Chita city (Fig. S1). The site was discovered by Sofia M. Sinitsa, and her team from the Institute of Natural Resources, Ecology, and Cryology, Siberian Branch of the Russian Academy of Sciences, while they were conducting a geological survey in the Olov Depression along the small Kulinda River, close to Chernyshevsk village. Four trenches were opened in the lower part of the Ukureyskaya Formation. This formation consists of massive and alternating sandstones, siltstones, tuffaceous sandstones, tuffaceous siltstones, and tuffites. Based on comparisons of the paleoentomological and the microfaunal contents with the Glushkovo Formation in the Unda-Daya Depression, the Ukureyskaya Formation has been dated as Late Jurassic – Early Cretaceous (*29, 30*). However, recent K-Ar dating suggests a slightly older age: the entire Ukureyskaya Formation ranges between 169 and 144 Ma (*29*), corresponding to a Bajocian-Tithonian age (Middle to Late Jurassic) (*31*). Two bonebed horizons have been excavated at the Kulinda locality, one in each of trenches 3 and 4. The two bonebeds are situated at 700 m and 680 m A.S.L., respectively, on the southern slope of a hill, and are separated laterally by 130 m; beds 3 and 4 lie beneath 1.0 - 1.5 m of colluvium and dip 28 and 22 degrees to the south'.

Bonebed 3, in trench n°3, is 10-20 cm thick and consists of well-preserved isolated bones within a gray, silty matrix (Figs. S2a, S3). Articulated elements and integumentary structures are rare.

The sediments in trench n° 4 are probably slightly older than those in trench n° 3. The bonebed comprises a finely laminated, organic-rich claystone and is completely devoid of dispersed quartz grains (Fig S2b-c, S3). Some of the bones in this horizon are articulated and delicate integumentary structures are preserved as a thin layer of carbon. It is clear that this horizon was deposited in a very calm environment, far from clastic sources. The matrix of this bonebed is highly indurated, and laminae are occasionally deformed; some skeletal elements are preserved as external molds. This contrasts with the lithology and style of preservation of the material from bonebed 3 and suggests localized chemical environments during diagenesis.

Both bonebeds are here regarded as monospecific: comparisons of the different skeletal elements within and between the two bonebeds do not provide any indication that more than one basal ornithischian is represented in the Ukureyskaya Formation of the Kulinda locality. Each

individual skeletal element is represented by a single morphotype and all the observed differences can easily be explained by ontogenetic and normal intraspecific variations, as confirmed by the detailed study of the partly articulated skeletons. Besides the basal ornithischian remains, a single shed tooth from a medium-sized theropod was found in bonebed 3. Only a total area for both bonebeds of about 200 m², which extends below the hill, has been investigated so far. It is therefore very difficult to estimate their total extent, and therefore, the minimum number of specimens present in the locality. More detailed sedimentological, geochemical, and taphonomic investigations are required in order to understand the quite unusual reservation of the fossils.

Systematic paleontology

<div align="center">

Dinosauria Marsh, 1881
Ornithischia Seeley, 1887
Neornithischia Cooper, 1985
Kulindadromeus zabaikalicus gen. et sp. nov.

</div>

Etymology. *Kulinda*, type locality; *Dromeus*, Greek for runner; *zabaikalicus*: from Zabaikal krai (region), where this new dinosaur was discovered.
Holotype. Institute of Natural Resources, Ecology and Cryology, Siberian Branch of the Russian Academy of Sciences, Chita, INREC K3/109, a partial skull (Fig. 1a, b).
Locality and horizon. Kulinda, Olov Depression, (Cherynyshevsky District of Chita Region, southeastern Siberia, Russia; Fig. S1); base of the Ukureyskaya Formation, Middle to Late Jurassic.
Diagnosis. Maxilla with rostral ascending process much lower than caudal ascending process and maxillary fenestra larger than antorbital fenestra; jugal with notched postorbital ramus; postorbital with dorsoventrally expanded caudal ramus; dorsoventrally slender postacetabular process on ilium; deep extensor fossae on metatarsals II-IV.

Osteological Description

This description is based on the material discovered between 2010 and 2012. A more detailed osteological description of *Kulindadromeus* will be published elsewhere, after preparation of the abundant material collected during the 2013 field season. The majority of the fossils discovered in bonebeds 3 and 4 belong to small individuals, likely juveniles or sub-adults; larger individuals are rare. The overrepresentation of younger individuals in the bonebeds could suggest an attritional accumulation of carcasses leading to the formation of the bonebeds, and not a single catastrophic event (*32*). However, a detailed age-frequency distribution of the long bones and further taphonomic investigations need to be conducted in order to confirm this hypothesis.

Skull
The description of the skull of *Kulindadromeus* is based on the study of six incomplete skulls, including the holotype INREC K3/109 (Fig. S4A, B), together with numerous disarticulated elements (Fig. S4C-G).
In lateral view, the skull of *Kulindadromeus* is triangular, closely resembling that of *Jeholosaurus* (*33*). The highest point of the skull is located above the orbit. Rostral to the orbit, the snout slopes ventrally without any significant changes in angle. Therefore, although it is incompletely preserved, it is likely that the preorbital region of the skull was relatively short,

accounting for approximately 50% of total skull length. The orbit is particularly large in INERC K3/109 (but it is probably an immature specimen) and has a subcircular outline in lateral view. The infratemporal fenestra is rostrocaudally narrow but dorsoventrally elongated; its ventral margin extends just beneath the orbit (Fig. S4A, B). The supratemporal fenestra appears rostrocaudally longer than mediolaterally wide.

Premaxilla **-** The premaxilla is fragmentary. Its lateral process is relatively long and, as in *Heterodontosaurus* (*34*) and *Jeholosaurus* (*33*), it contacts the lacrimal caudally, unlike in *Lesothosaurus* (*35*) and *Hypsilophodon* (*36*), in which the premaxilla and lacrimal are separated by the high rostral ascending process of the maxilla. At least three premaxillary teeth were present.

Maxilla **-** The maxilla is rostrocaudally elongated, but dorsoventrally low (Fig. S4D). It contains at least 19 teeth, larger specimens possessing more teeth. The tooth row is dorsally bordered by a salient horizontal crest, although there is apparently no true buccal emargination. The caudal part of the tooth-bearing ramus is ventrally inclined and tapers gradually towards its termination, with the sloping dorsal side of this ramus forming the contact region with the jugal. Rostral to the jugal contact, the maxilla forms a caudal ascending process, extensively covered by the lacrimal, with a broad base and a subtriangular outline in lateral view. The rostral ascending process, which contacts the lateral process of the premaxilla, is much less developed than the caudal ascending process, contrasting with the lower caudal process and the much higher rostral process in *Heterodontosaurus* (*34*), *Jeholosaurus* (IVPP V12530-V15716) and *Hypsilophodon* (NHM R2477). Between the ascending processes, the maxilla is deeply depressed to form the ventral part of the large (about 57% of orbital length), subelliptical and rostrocaudally-elongate antorbital fossa. The much smaller antorbital fenestra is confined to its caudal portion, not far from the lacrimal. A larger maxillary fenestra is present between the caudal border of the rostral ascending process and the lateral process of the maxilla. A separate maxillary fenestra is also reported in *Heterodontosaurus* (*34*), *Hypsilophodon* (*36*) and *Haya* (*37*), but unlike in *Kulindadromeus*, it remains smaller than the antorbital fenestra. A sulcus extends from the maxillary fenestra between the dorsorostral border of the rostral ascending process and the lateral process of the premaxilla, likely reflecting a slight ventral displacement of the maxilla rather than a true morphological feature.

Lacrimal **-** The lacrimal has the shape of an inverted 'L' in lateral view and consists of a ventral and a dorsal process (Fig. S4A, B). The dorsal border of the dorsal process contacts the prefrontal and the nasal and its tip contacts the lateral process of the premaxilla. Its ventral border participates in the dorsal margin of the antorbital fossa, but unlike in *Heterodontosaurus* (*34*), *Jeholosaurus* (*33*) and *Hypsilophodon* (*36*), it does not contact the rostral ascending process of the maxilla. The rostral border of the ventral process contacts the caudal ascending process of the maxilla, while its caudal end contacts the rostral process of the jugal. Its caudal border participates in the rostral margin of the orbit and contacts the palpebral.

Nasal **-** The nasals are relatively wide and form a broad roof over the snout, as in *Lesothosaurus* (*35*), *Jeholosaurus* (*33*) and *Haya* (*37*) (Fig. S4A, B). A midline depression is present along the internasal suture, as in basal neornithischians (*38*) and ornithopods such as *Jeholosaurus* (*33*), *Changchunsaurus* (*39*) and *Haya* (*37*). The caudolateral border of the nasal is overlapped extensively by the prefrontal. Caudally, the nasal contacts the frontal at the level of the rostral part of the orbit.

Frontal **-** The frontals are rostrocaudally elongated, forming an extensive skull table (Fig. S4A, B). However, they are less than twice as long as wide, contrasting with the proportionally longer and narrower frontals in *Jeholosaurus* (maximum length to width ratio of approximately

3.0, IVPP V15717), *Agilisaurus* (3.0, ZDM T6011), *Hypsilophodon* (3.2, NHM R197, NHM R2477), and *Zephyrosaurus* (MCZ432; 3.0), all specimens of similar size. Rostrally, the frontal contacts the nasal and the prefrontal at the level of the rostrodorsal angle of the orbit. The lateral border of the frontal participates in the dorsal margin of the orbit, and then it contacts the median ramus of the postorbital. Caudally, the suture with the parietal is relatively straight.

Parietal **-** The parietals remain unfused in INREC K3/109, without a salient sagittal crest (Fig. S4A, B), suggesting that it was an immature specimen. They bifurcate rostrally to meet the median process of the postorbital and participate in the rostral margin of the supratemporal fenestra. They also bifurcate caudally to meet the median process of the squamosal and contribute to the caudal margin of the supratemporal fenestra. The caudal edge of the parietals appears deeply notched at the midline as in *Jeholosaurus* (*33*) and *Haya* (*37*).

Squamosal **-** The squamosal consists of a central plate that supports four divergent processes (Fig. S4A, B). The postorbital process is dorsoventrally wide; it participates in the caudolateral margin of the supratemporal fenestra and contacts the caudal process of the postorbital. The medial process is relatively elongated; it contacts the parietal medially and participates in the caudal margin of the supratemporal fenestra. Both the pre- and postcotyloid processes are long and slender, and they taper distally. The postcotyloid process is longer and more robust than the precotyloid process. Together, they limit a deep semicircular cotylus for the proximal articular head of the quadrate.

Postorbital **-** The postorbital is a triradiate bone (Fig. S4A, B). The caudal process, which contacts the squamosal, is rostrocaudally short, but appears dorsoventrally higher than in other basal ornithischians and ornithopods. The median process is rather long and contacts medially the frontal and the parietal. The ventral process is long, rostrally inclined, and tapers distally to insert into the bifid postorbital process of the jugal. The caudal border of the median process and the dorsal border of the caudal process form the rostral margin of the supratemporal fenestra. The rostral margin of the ventral process and the rostral margin of the median process form the caudodorsal corner of the orbit. The ventral border of the caudal process and the caudal border of the ventral process participate in the rostral margin of the infratemporal fenestra.

Jugal **-** The jugal is a strap-like triradiate bone that forms the ventral borders of both the orbit and infratemporal fenestra (Fig. S4A, B). The maxillary process is elongated and rod-like. Its ventral border contacts the maxilla and its tip contacts the lacrimal. As in *Hexinlusaurus* (*38*) and all basal ornithopods including *Orodromeus* (*40*), the jugal does not contribute to the margin of the antorbital fossa. Unlike in *Hypsilophodon* (*36*), the quadratojugal process is well developed. Unlike in *Lesothosaurus* (*35*), *Heterodontosaurus* (*34*), *Jeholosaurus* (*33*), *Haya* (*37*), *Psittacosaurus* (*41*) and possibly *Changchunsaurus* (*39*), its caudal end is not bifid. The postorbital process is robust and slightly inclined caudally. Its tip is bifid, forming a deep cotylus for reception of the ventral end of the jugal process of the postorbital. The caudal ramus of the fork is much higher than the rostral ramus.

Quadratojugal **-** Located between the quadratojugal and the postorbital ramus of the jugal, the quadratojugal is not dorsally expanded, in contrast to *Hypsilophodon* (*36*), leaving a dorsoventrally higher infratemporal fenestra (Fig. S4A, B). The ventral contact with the jugal appears particularly complex, but cannot be adequately described because of the poor preservation of the specimen. A small foramen is apparently present at the junction between the quadratojugal and the jugal, contrasting with the large quadratojugal foramen that pierces the centre of the quadratojugal in *Hypsilophodon* (*36*), *Jeholosaurus* (*33*), and *Haya* (*37*). This paraquadratic foramen is apparently absent in *Lesothosaurus* (*35*), *Heterodontosaurus* (*34*), and *Orodromeus* (*40*). Caudoventrally, the quadratojugal extends very close to the quadrate condyles.

This is similar to the condition in most basal cerapodans, including *Hypsilophodon* (*36*), *Jeholosaurus (33)*, *Changchunsaurus* (*39*), *Haya* (*37*), *Orodromeus* (*40*) and *Psittacosaurus* (*41*), but differs from the condition in more advanced ornithopods in which the dorsoventral extent of the quadratojugal is reduced and the ventral margin does not approach the quadrate condyles (*42*).

Quadrate **-** The quadrate is proportionally high and rostrocaudally slender, although it does not extend ventrally as far as in *Hypsilophodon* (*36*), so only a small part of the quadrate is below the level of the maxilla (Fig. S4A, B). The quadrate shaft is distinctly curved backwards in lateral view, so that its dorsal contact with the squamosal is located caudal to the level of the quadrate condyles. However, the caudal deflection of the proximal head of quadrate is not as pronounced as in *Hypsilophodon* (*36*), *Changchunsaurus* (*39*), and *Zephyrosaurus* (*43*), in which the proximal head of the quadrate is caudally deflected from the shaft. The lateral surface of the quadrate appears depressed, as is also typical in basal ornithopods (*42*).

Palpebral **-** The palpebral is particularly long, likely extending along more than 75% the diameter of the orbit and appears triradiate. Its base is dorsoventrally enlarged, whereas its caudal end is particularly acute (Fig. S4A, B).

Dentary **-** The dentary is rostrocaudally elongate and dorsoventrally low (Fig. S4A, B). As in *Changchunsaurus* (*39*) and *Haya* (*37*), a slightly everted area borders the first two or three alveoli on the lateral side of the dentary. The lateral surface of the dentary is slightly convex dorsoventrally, as in most ornithischians. Its dorsal part forms a slight buccal emargination, limited ventrally by a low ridge. A series of small foramina opens along this ridge. The dorsal height of the buccal emargination appears constant. More than 17 dentary teeth appear to have been present in INREC K3/112. The ventral part of the medial surface of the dentary has a well-defined horizontal line of small nutrient foramina.

Surangular **-** The surangular is rather short and robust. There is apparently no foramen on the lateral side of the surangular, adjacent to the contact with the dentary (Fig. S4A, B), unlike in basal ornithopods, including *Hypsilophodon* (*36*), *Orodromeus* (*40*), *Jeholosaurus* (*33*), *Changchunsaurus* (*39*), and *Haya* (*37*). Because the dorsal part of the surangular is hidden by the jugal in INREC K3/109, it is not possible to observe whether an unciform process is developed adjacent to the glenoid, as in *Hypsilophodon* (*36*), *Orodromeus* (*40*), *Changchunsaurus* (*39*), *Haya*, and *Thescelosaurus* (*37*). The glenoid part of the surangular appears particular long and slender in lateral view. The retroarticular process is quite rudimentary.

Angular **-** The angular is displaced in INREC K3/109. It is a flat and elongated bone along the ventral portion of the posterior mandibular ramus, extending below the glenoid and the coronoid process (Fig. S4A, B), as in other basal ornithopods (*42*).

Splenial **-** The splenial is a sheet-like bone that covers most of the medial surface of the caudal dentary, as in *Changchunsaurus* (*39*). Its height regularly decreases rostrally, terminating ventral to the fourth dentary tooth (Fig. S4F). The splenial foramen is proportionally much larger than in *Changchunsaurus* (*39*) and *Haya* (*37*).

Dentition **–** The preserved premaxillary teeth are pointed, slightly recurved and apparently unserrated, as is usually observed in basal Ornithischia and Ornithopoda (*42, 44*). The roots of the maxillary teeth are closely packed, high and cylindrical in cross-section. The maxillary crowns are too poorly preserved in the material currently unearthed from the Kulinda locality to be adequately described.

The root of the dentary teeth is high, labiolingually compressed and trapezoidal in lingual view. Unlike in Heterodontosaurinae (*34*), the crown is proportionally low, about one third of the root height. The root and the crown are separated by a shallow constriction. As in

Heterodontosaurus (*34*) and *Hypsilophodon* (*36*), the first dentary teeth appear to have a simpler and more conical crown, but the crowns of the other teeth are labiolingually compressed, with denticulate edges. The enamel layer appears thicker on the lingual side, forming a cingulum–like swelling at the base of the lingual side. The labial side usually forms a single obliquely inclined, planar wear facet. The edge of the crown is slightly asymmetrical in lingual view, forming six or seven coarse denticles. The largest denticle is the third one. The lingual side of the dentary crowns is devoid of a median vertical eminence (Fig. S4F-G), unlike in *Orodromeus* (*40*), *Changchunsaurus* (*39*), and *Haya* (*37*) and of vertical ridges, unlike in *Hypsilophodon* (*36*), *Haya* (*37*), *Zephyrosaurus* (*43*), *Thescelosaurus* (*45*), and *Bugenasaura* (*46*). The dentary crowns overlap one another in an imbricate fashion: the distal part of each crown laterally overlaps the mesial part of the succeeding crown (Fig. S4E, G), as also described in *Hypsilophodon* (*36*), *Orodromeus* (*40*), and *Changchunsaurus* (*39*).

Postcranial Skeleton

Axial skeleton – Few elements from the axial skeleton have been recovered at the Kulinda locality so far. Only one dorsal vertebra can be observed in lateral view (Fig. S5A), but its transverse process is broken off. Its neural spine appears proportionally taller, but less elongated craniocaudally than in *Hypsilophodon* (*36*) and, especially, *Haya* (*37*).

Four proximal caudal vertebrae are preserved in articulation in INREC K4/150, in lateral view (Fig. S5C). Their centrum is slightly longer than high, with a markedly concave ventral surface between the prominent chevron facets, as also observed in *Hypsilophodon* (*36*) and *Haya* (*37*). The chevron facets of adjacent centra form a deep inverted V-shaped articulation area for the chevrons.

The most complete caudal series is present in INREC K4/159, which has 11 distal caudal vertebrae preserved in articulation, in lateral view (Fig. S5D). The centra are particularly elongate, being at least twice as long as they are high. Their ventral surface is very concave in lateral view. The neural arch is absent or too low to be observable in lateral view. Both the pre- and postzygapophyses become very elongate and extend well beyond the proximal or distal limits of the centrum (Fig. S5B) and exhibit considerable overlap. The articular facets of the zygapophyses are almost vertically inclined, as also observed in the distal caudal vertebrae of *Jeholosaurus* (*33*). There is no trace of ossified tendons.

Scapula – The proximal plate of the scapula is less expanded dorsoventrally than in *Koreanosaurus* (*47*) and *Changchunsaurus* (*48*). The acromial process is very prominent, although less developed than in *Orodromeus* (*40*) and *Oryctodromeus* (*49*) (Fig. S6B). The sutural surface for the coracoid is straight and much wider than the glenoid. The shaft of the scapular blade immediately distal to the proximal plate is dorsoventrally narrow; the scapula length is about 8.3 times the height of the minimum dorsoventral height of the blade (Fig. S6A). The dorsal margin of the scapular blade remains straight, whereas its ventral margin expands strongly distally; as a result, the distal end of the scapular blade is strongly asymmetrically expanded and is more than two times the height of the scapular neck in smaller specimens. The scapular blade appears ontogenetically more expanded, being more than three times the height of the scapular neck in larger specimens.

Humerus – The humerus is longer than the scapula. Its proximal end is mediolaterally expanded and craniocaudally compressed (Fig. S6A). The deltopectoral crest is prominently expanded laterally. It is not turned cranially as in *Hypsilophodon (36)* and *Orodromeus* (*40*). It is however less developed than in *Koreanosaurus* (*47*) and its base does not reach the mid-length of the bone. The medial border of the humerus is regularly concave along its whole length. The

humeral shaft is relatively narrow. The distal portion of the humerus is slightly twisted medially and is less mediolaterally widened than in *Koreanosaurus* (*47*). The ulnar condyle is better-developed mediolaterally than the radial condyle.

Ulna – The ulna is rather robustly built and apparently bowed ventrally (when oriented horizontally; Fig. S6C). Therefore, it is likely that a wide gap separated the ulna and the radius, allowing for some ability for pronation/supination of the manus with respect to the upper arm. Its proximal end is mediolaterally enlarged and triangular in cross section. Its dorsal side forms a wide and flat articulation area for the proximal part of the radius. The olecranon process is weakly developed as is usual in basal ornithopods. The ulnar shaft progressively tapers distally, but the distal end of the ulna is again enlarged mediolaterally, forming a well-defined articulation area for the distal end of the radius.

Ilium – The preacetabular process is about 40% of the ilium length, dorsoventrally narrow and strongly deflected ventrally, reaching the level of the pubic peduncle (Fig. S7A). The postacetabular process is 36% of the ilium length and is particularly narrow dorsoventrally. Its dorsal border is straight and its lateral side faces slightly dorsally. Its dorsolateral side has a slightly developed supraacetabular crest. Unlike in Cerapoda, the pubic peduncle is prominent, triangular in lateral view; it forms a 45° angle with the craniocaudal axis of the ilium body (*16*). The ischiac peduncle projects ventrally and is stouter than the pubic peduncle. The acetabulum is deep and semi-circular, without any trace of a supraacetabular flange and of a medioventral acetabular flange. The posterior portion of the brevis shelf cannot be observed in lateral view.

Pubis – The prepubic process is elongated and rod-like (Fig. S7B); although it appears proportionally shorter than in *Hypsilophodon*, the prepubic process likely extended beyond the preacetabular process of the ilium. The body of the pubis is particularly wide and participated in an important portion of the acetabulum. The iliac peduncle is wide and continuous with the slender, hook-shaped ischial peduncle that partially encloses the obturator notch. The pubic shaft is relatively long, slender, and curved dorsally. Along the dorsal border of the pubic shaft, a well-developed triangular obturator process partially encloses the obturator notch. The presence of an obturator notch or foramen appears to be subject to intraspecific variation in *Hypsilophodon* (*36*): an obturator notch is present in some individuals (NHM R195, R5829), while a foramen is present in others (NHM R193, R196).

Ischium – The proximal ischial head is separated from the large flat blade region by a constricted shaft (Fig. S7C). The iliac peduncle is slightly larger than the pubic peduncle; both processes are separated by a deep acetabular notch. The angle between the ischial head and shaft is more pronounced than in other basal ornithischians and ornithopods described so far, so that the ischium appears more curved dorsally. The ischial blade is mediolaterally compressed and curved dorsally, parallel to the pubic shaft. A tab-like obturator process is developed along its ventral margin, distal to the ischial neck.

Femur – Femora are very fragmentary in the bonebeds studied herein. The femoral head is prominent and supported by a long neck (Fig. S7F). The femoral head and shaft form an angle of about 100°-110° and the top of the femoral head is set above the greater trochanter. The femoral shaft appears relatively long, slender and curved slightly caudally. The 4th trochanter is set on the proximal part of the femoral shaft (Fig. S7D). Although it is incompletely preserved, it looks particularly robust and roughly triangular in lateral view, contrasting with the more slender, pendant 4th trochanter in other basal Ornithischia or Ornithopoda. The femoral shaft is slender and appears bowed in medial or lateral view. The distal portion of the femur is mediolaterally widened. The medial and lateral condyles are not well developed.

Tibia – The tibia is much more slender in proportion to its length than in *Hypsilophodon* (*36*), more closely resembling the situation in *Heterodontosaurus (34)*. As is usual in basal Ornithischia, the cnemial crest is poorly developed; it projects anterolaterally in smaller specimens, but more steeply laterally in larger ones (Fig. S7G). A deep, proximodistally-extending *incisura tibialis* separates the cnemial crest from the prominent fibular condyle. A prominent accessory condyle is developed between the fibular condyle and the cnemial crest. At the proximodorsal corner of the tibia, the inner condyle is widely developed above the tibial shaft. A broad notch separates the inner and fibular condyles from one another. The tibial shaft is long, straight, and particularly slender (Fig. S7E). The distal part of the tibia is slightly expanded mediolaterally to form the distal malleoli and its flattened cranial surface forms an extended surface against which the ascending process of the astragalus articulated. The distal malleoli are not particularly salient; the inner malleolus is more robust than the outer one.

Fibula – The proximal portion of the fibula is craniocaudally enlarged, but mediolaterally compressed, with a slightly convex lateral side. The shaft is proportionally extremely slender and perfectly straight.

Metatarsals – Metatarsal I is proportionally long (about 80% metatarsal II length) and robust (Fig. S7H, I). Its proximal end is mediolaterally expanded, as in *Heterodontosaurus* (*34*), and unlike the splint-like metatarsal I in *Changchunsaurus* (*48*), *Jeholosaurus* (*50*), *Orodromeus* (*40*), and *Othnielosaurus* (*42*). Its lateral side is concave, where it was closely appressed to metatarsal II. Its distal end is expanded both mediolaterally and craniocaudally, forming a single articular condyle with a convex articular surface.

Metatarsal II is longer than metatarsal IV, but shorter than metatarsal III (Fig. S7H, I). In dorsal view, its medial side is regularly concave, whereas its lateral margin forms a strong crest that partially covers the dorsal side of metatarsal III. Its dorsal side is flattened, except along its distal quarter, where it forms a long and deep extensor fossa, suggesting important hyperextension for digit II. Its distal end is expanded into a bicondylar articular surface, with well-developed collateral ligament pits.

Metatarsal III is the longest of the series. It is nearly perfectly straight (Fig. S7H, I). Its proximal end is transversely compressed and expanded dorsoventrally with a quadrangular outline. Distally, metatarsal III expands dorsoventrally and transversely to form two well-defined condyles. The extensor fossa on its dorsal side is deep, although less extended than on metatarsal II and IV.

The shaft of metatarsal IV is closely appressed to metatarsal III; however, at its distal end, it diverges laterally, away from metatarsal III (Fig. S7H, I). Its distal articulation is strongly expanded mediolaterally and is wider than the distal articulation of metatarsals II and III. The extensor fossa is also wider, indicating that hyperextension of digit IV was particularly important. The collateral ligament pits are also deeper than on metartarsals II and III.

Pes phalanges – Digit I is composed of two phalanges. Phalanx I-1 is relatively long and very slender; it extends well beyond the distal end of metatarsal II. Phalanx I-2 is a tiny triangular element. Phalanges II-1 and III-1 are robust and elongated. Their proximal articular surface is expanded both dorsoventrally and mediolaterally; it is subdivided into two concavities by a median ridge. Their distal articular surface is very convex and clearly bicondylar, with deep collateral ligament pits. Phalanx IV-1 is much smaller, but has a similar morphology; a well-developed flexor tubercle is present along the ventral margin of its proximal articular surface, at the base of the median ridge. Digit IV is composed of four phalanges. Phalanges IV-1 to IV-4 have a similar morphology, but their size gradually decreases throughout the series. The ungual

phalanges of digits 2 and 3 are elongate with deep lateral ligament grooves and sharp distal ends. Traces of the claw sheath are preserved in some isolated ungual phalanges.

Notes on the Integumentary Structures in *Kulindadromeus*

The mode of preservation of the described integumentary structures - i.e. preservation as dark carbonaceous films - is identical to that of all other examples of filamentous integumentary structures in dinosaurs from the Jehol Biota in northeastern China. The preservation of these carbonaceous films as the degraded remains of feather-like filamentous structures or 'protofeathers' is not universally accepted, some authors arguing that the so-called downy 'protofeathers' in *Sinosauropteryx* or the bristle-like structures in *Psittacosaurus* are in fact degraded remains of collagen fibers (*2, 4, 51*). Therefore, it might also be hypothesized that the filamentous structures around the bones of *Kulindadromeus* also represent degraded collagen fibers. However, we argue that this hypothesis is unlikely for several reasons. First, integumentary collagen fibers typically occur in layered arrays of parallel, densely packed fibers where fibers in successive layers are oblique to one another. The filamentous structures described herein, however, are organized into discrete, regularly spaced clusters and there is no evidence for arrangement of fibers into successive vertical layers; it is difficult to envisage how such an arrangement could be generated during decay of collagen. Second, integumentary collagen fibers are typically on the order of several microns in diameter; the structures we describe are at least two orders of magnitude larger. Thirdly, the morphology of the compound and ribbon-like integumentary filaments (Fig. 3D-H) is unknown for integumentary collagen.

Given that plant remains are abundant in the lithological beds above and below bonebed 4 (but not in bonebed 4 itself), it could be argued that the filamentous and compound structures found in bonebed 4 represent in fact vegetal remains. Plant debris in similar lithologies and depositional settings typically exhibits a random distribution and orientation. However, the structures described herein are systematically associated with skeletal elements, regularly spaced, aligned and orientated consistently with respect to the limb bones. Therefore, these observations argue strongly against any hypothesis that the structures are of plant origin. Further, several paleobotanists (E. Bugdaeva, Sun Ge, C. Prestianni, pers. comm.) have examined the carbonaceous filaments associated with *Kulindadromeus*, but failed to identify any evidence for a vegetal affinity for these structures.

We considered attempting to describe the feather morphotypes in *Kulindadromeus* using the nomenclature of Prum et al. (*52, 53*) or of Xu et al. (*21, 22*). However, except for our monofilaments (which correspond well to Type 1 in Xu et al.), we could not assign with confidence the other two feather morphotypes in *Kulindadromeus* to categories described by Prum et al. or Xu et al. Further, fundamental discrepancies between these two previously published nomenclature systems remain to be resolved. Thus we felt that until new fossil material and a synthesis of existing nomenclature systems are available, interpretations of direct homologies between complex feather-types in *Kulindadromeus* and in Prum et al. or Xu et al. would be premature.

Phylogenetic analysis

To assess the phylogenetic position of *Kulindadromeus zabaikalicus*, we included this new taxon in the most recent and comprehensive phylogeny of ornithischian dinosaurs (*50*). We did not include the taxa *Yandusaurus*, *Anabisetia*, *Echinodon*, *Yueosaurus*, and *Koreanosaurus* in the analysis, because they were regarded as unstable 'wildcard' taxa in the original analysis (*50*). In the course of the analysis, we subsequently deleted *Othnielosaurus consors*, regarded as another

'wildcard' taxon. Excluding 'wildcard' taxa, the resultant data matrix consists of 227 characters and 48 taxa. Five characters (112, 135, 137, 138, and 174) were treated as ordered (*50*). The data matrix was analysed using the TNT 1.1 software package (*54*). A heuristic search of 10000 replicates using random addition sequences, followed by branch swapping by tree-bisection-reconnection (TBR; holding ten trees per replicate), was conducted. The trees were subsequently analysed using Winclada ver.1.00.08 (*55*) with fast and slow optimizations. To assess the repeatability of tree topologies, a bootstrap analysis was performed (1000 replicates with the heuristic algorithm in Winclada). Bremer support was assessed by computing decay indices with TNT 1.1.

Heuristic searches recovered four most parsimonious trees (MPTs) of length 571 steps, with a Consistency index (CI) excluding uninformative characters = 0.42, and a Retention index (RI) = 0.67. The strict consensus tree (Fig. S10) shows that *Kulindadromeus* is the sister taxon of Cerapoda (*Parasaurolophus walkeri* Parks, 1922, *Triceratops horridus* Marsh, 1889, their most recent common ancestor and all descendants; *16*). They share the following unambiguous synapomorphies: length of the postacetabular process more than 35% of the length of the ilium (character 174 [2]), medioventral acetabular flange of ilium absent (character 175 [1]), and fossa trochanteris modified into a distinct constriction separating the head and the greater trochanter on the femur (character 198 [1]). These three synapomorphies are absent in *Agilisaurus louderbacki* and *Hexinlusaurus multidens*, the closest relatives of *Kulindadromeus* and Cerapoda from the Middle Jurassic of Sichuan Province in China (*16*). Unlike in typical Cerapoda, apicobasally extending ridges on the lingual/labial surfaces of the maxillary/dentary crowns confluent with the marginal denticles are absent in *Kulindadromeus* (character 119 [0]), its humerus is substantially longer than its scapula (character 119 [1], reversion in Cerapoda), and the pubic peduncle of its ilium is large, elongate, and robust (character 178 [0]).

It should be noted that this phylogenetic hypothesis is only weakly supported by the available data. Bremer support and bootstrap values for the recovered ornithischian subclades are, in general, low. This low support is partly caused by various homoplasies (some of which are functionally significant), which are distributed widely across ornithischian phylogeny.

When the phylogeny (Fig. S10) is plotted against geological time (Fig. S11), it can be seen that, despite its basal phylogenetic position, *Kulindadromeus* is part of a small group of similarly aged outgroups to Cerapoda. The phylogeny and stratigraphic ordering are broadly congruent.

Matrix. Our phylogenetic analysis is based on a matrix published in a recently published phylogeny of Ornithischia (*50*). The updated character scores for *Kulindadromeus zabaikalicus* are indicated below:

??????1????1?0??????001?01?010?001???000000000000011000??0011?000? 00??000????????????01?????1000?1?10?00000???11000?0?000011110??? ???????0??????1010?01????????010?0?0??121100000??1?110?00111??01??2 0???1???000??00??000?00??1

List of synapomorphies supporting selected nodes shared by all most parsimonious trees. Character numeration refers to the Character list in a recently published phylogeny of Ornihischia (*50*). Transformation was evaluated under accelerated transformation (ACCTRAN) and delayed transformation (DELTRAN) options; unambiguous synapomorphies are those that diagnose a node under both ACCTRAN and DELTRAN optimization. Node enumeration refers to Figure S10.

Neornithischia: Unambiguous: 184 (0→1); ACCTRAN: 46 (1→0), 52 (0→1), 75 (0→1), 92 (0→1), 101 (0→1), 104 (0→1), 106 (1→0), 133 (0→1), 185 (0→1)

Node B: Unambiguous: 149 (0→1); 194 (0→1); DELTRAN, 46 (1→0), 75 (0→1), 101 (0→1), 104 (0→1), 106 (1→0), 133 (0→1).

Node C: Unambiguous: 34 (0→1), 173 (0→1), 176 (0→1), 183 (1→0), 193 (0→1), 195 (0→1), 209 (0→1); ACCTRAN: 63 (1→0), 91 (0→1), 95 (0→1), 211 (1→0); DELTRAN: 185 (0→1).

Node D: Unambiguous: 174 (1→2), 175 (0→1), 198 (0→1); ACCTRAN: 138 (2→3), 139 (0→1), 199 (2→3), 200 (0→1); DELTRAN: 52 (0→1), 211 (1→0).

Cerapoda: Unambiguous: 119 (0→1), 149 (1→0), 178 (0→1); ACCTRAN: 22 (0→1), 177 (0→1); DELTRAN: 91 (0→1), 92 (0→1), 138 (2→3), 139 (0→1), 199 (2→3), 200 (0→1).

Marginocephalia: Unambiguous: 41 (0→1), 68 (0→1), 84 (0→1), 112 (1→3), 150 (0→1), 184 (1→0), 188 (0→1), 193 (0→2), 203 (0→1); ACCTRAN: 19 (1→0), 34 (1→0), 72 (0→1), 81 (0→1), 108 (0→1), 117 (0→1), 136 (0→1), 137 (1→0), 147 (0→1), 168 (0→1), 169 (0→1), 180 (0→1).

Ornithopoda: Unambiguous: 13 (0→1), 64 (0→1), 105 (0→1); ACCTRAN, 122 (1→0), 145 (0→1), 189 (1→0); DELTRAN: 22 (0→1), 63 (1→0), 177 (0→1).

Institutional abbreviations

INREC, Institute of Natural Resources, Ecology and Cryology, Siberian Branch of the Russian Academy of Sciences, Chita, Russia; IVPP, Institute of Vertebrate Paleontology and Paleoanthropology, Beijing, China; MCZ, Museum of Comparative Anatomy, Harvard University, USA; NHM, Natural History Museum, London, UK; ZDM, Zigong Dinosaur Museum, Dashanpu, China.

Fig. S1. Location of Kulinda dinosaur locality. Inset map: Zabaikalsky Krai (in yellow).
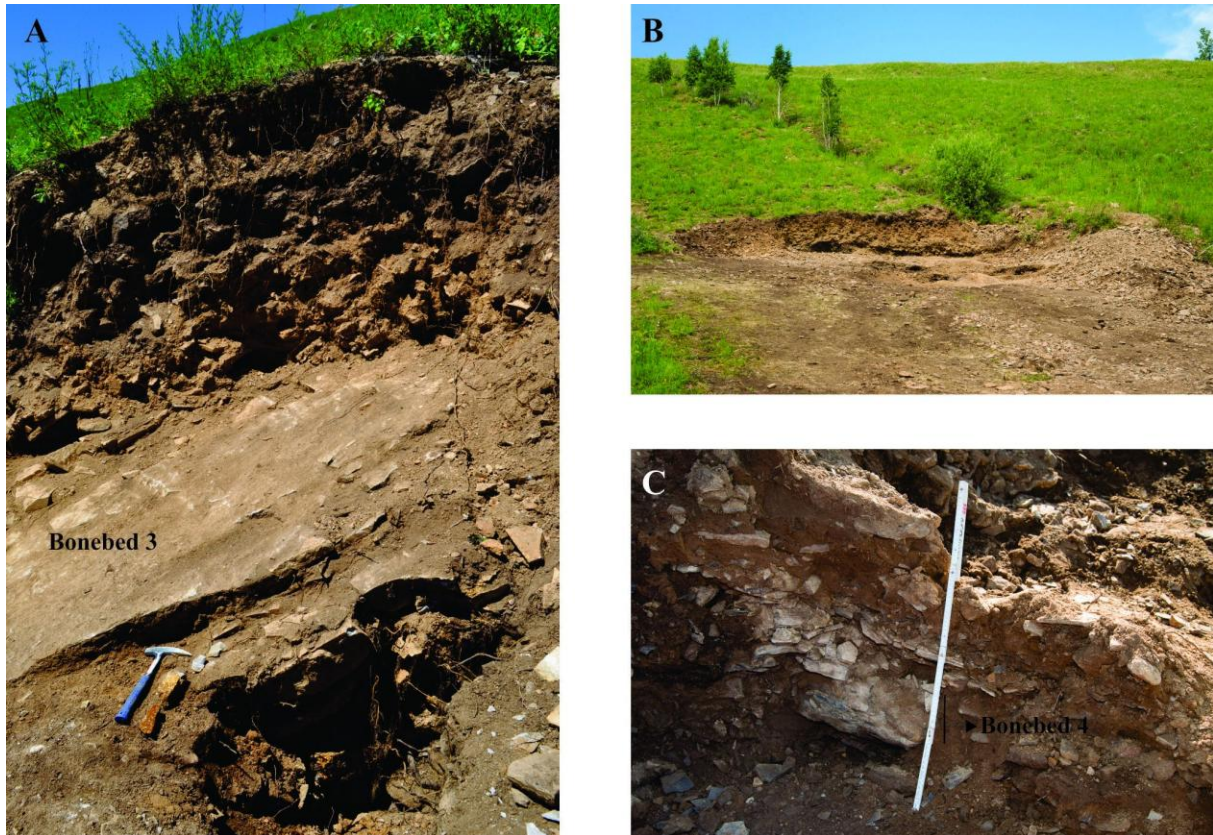
Fig. S2. The Kulinda dinosaur locality, Ukurey Fm (Middle to Late Jurassic) of Kulinda (Chitinskaya Oblast, Russia). A, Photograph of the b3 excavation (view to the west); B, b4 excavation (general view to the north), the position of trench 4 is located along the alignment of the trees in the image; C, bonebed 4 in the south front of the b4 excavation. Backfills overlying the bonebeds are being removed (view to the south).
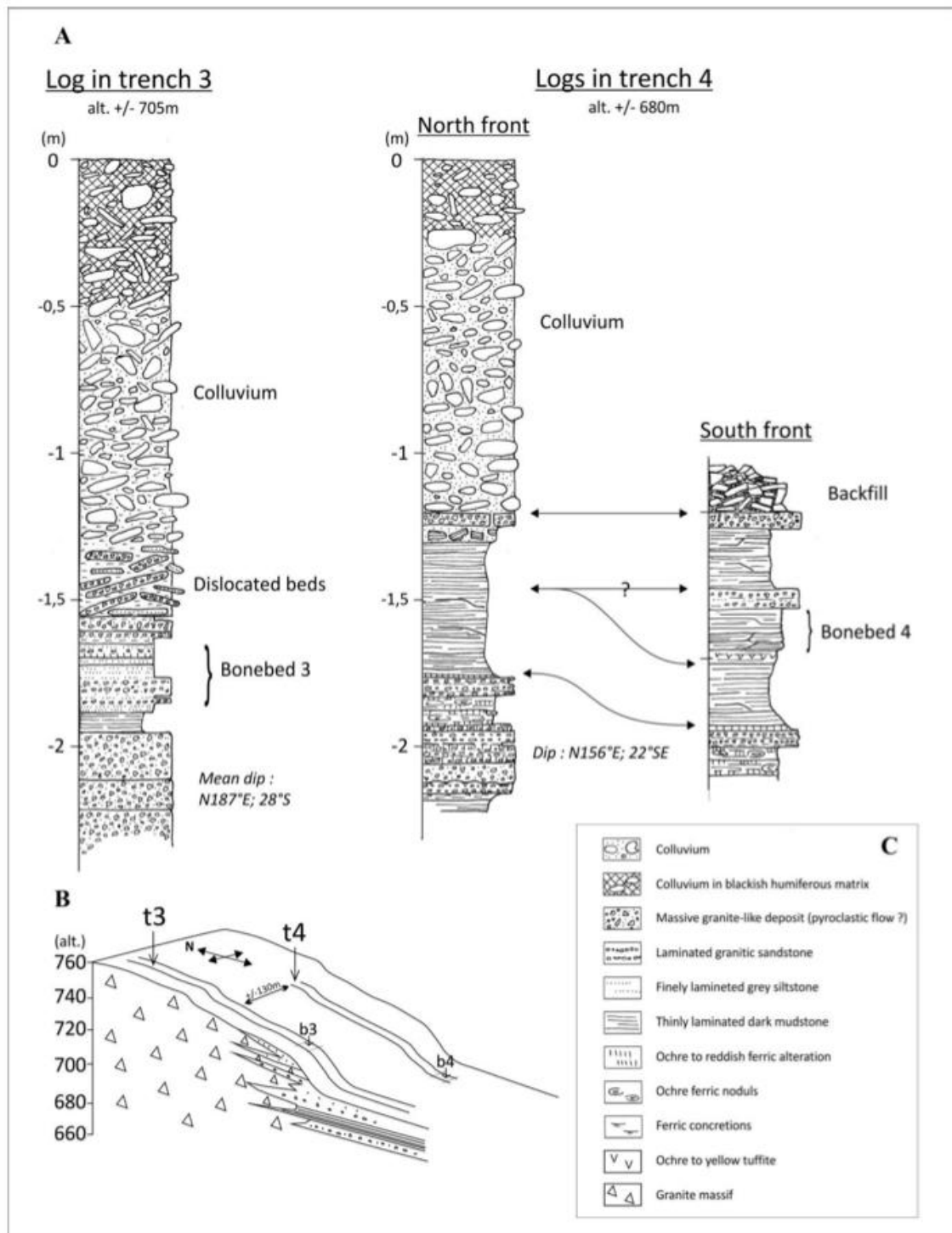
Fig. S3. Lithological log of the Kulinda dinosaur locality, Ukurey Fm (Middle to Late Jurassic). The log is taken from the sediments in trench 3 and 4, with the positions of the bonebeds. Bonebed 4 was only crossed in the south front of the trench 4 excavation; B, schematic positioning of the trenches (T3 and T4) and of the excavations (b3 and b4); C, lithological legend of the figures.
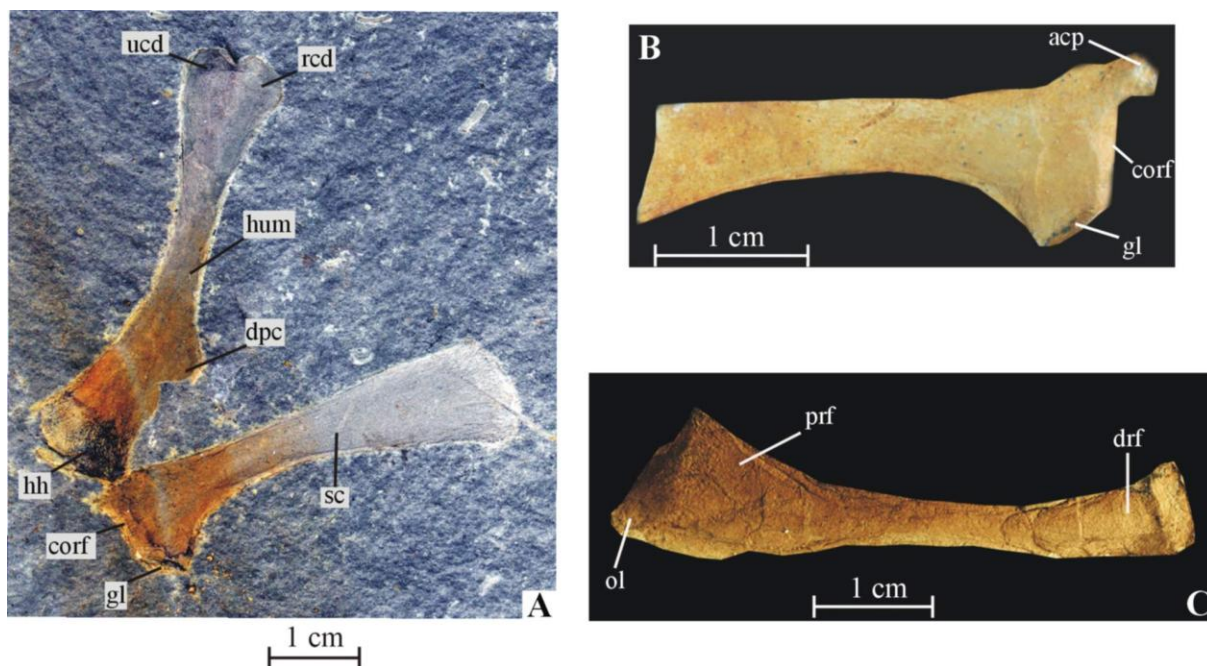
16
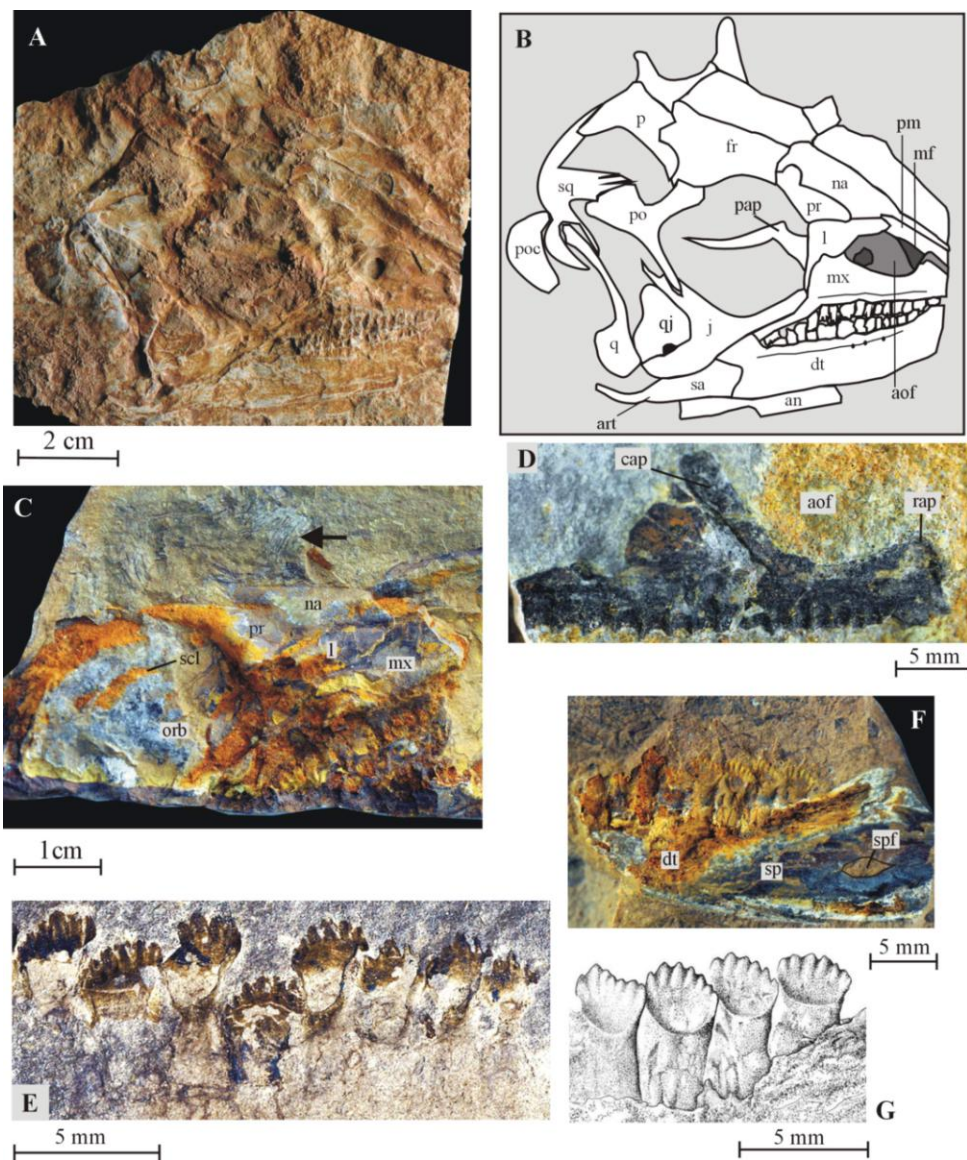
Fig. S4. *Kulindadromeus zabaikalicus* **nov. gen., nov. sp., from the Ukurey Fm (Middle to Late Jurassic) of Kulinda (Chitinskaya Oblast, Russia).** Photograph (**A**) and line drawing (**B**) of the holotype skull (INREC K3/109) in right lateral view; **C**, partial skull (INREC K4/22) in right lateral view, note the presence of monofilaments above the orbital region; D, right maxilla (INREC K4/42) in lateral view; **E**, dentary teeth (INREC K3/200) in lingual view; **F**, right dentary ramus (INREC 4/201) in lingual view. **G**, dentary teeth (INREC 3/200) in lingual view. Abbreviations: an, angular; aof, antorbital fossa; art, articular; cap, caudal ascending process; dt, dentary; fr, frontal; j, jugal; l, lacrimal; mf, maxillary fenestra; mx, maxilla; na, nasal; orb, orbit; p, parietal; pap, palpebral; pm, premaxilla; po, postorbital; poc, paroccipital process; pr, refrontal; q, quadrate; qj, quadratojugal; rap, rostral ascending process; sa, surangular; scl, scleral plates; sp, splenial; spf, splenial foramen; sq, squamosal.
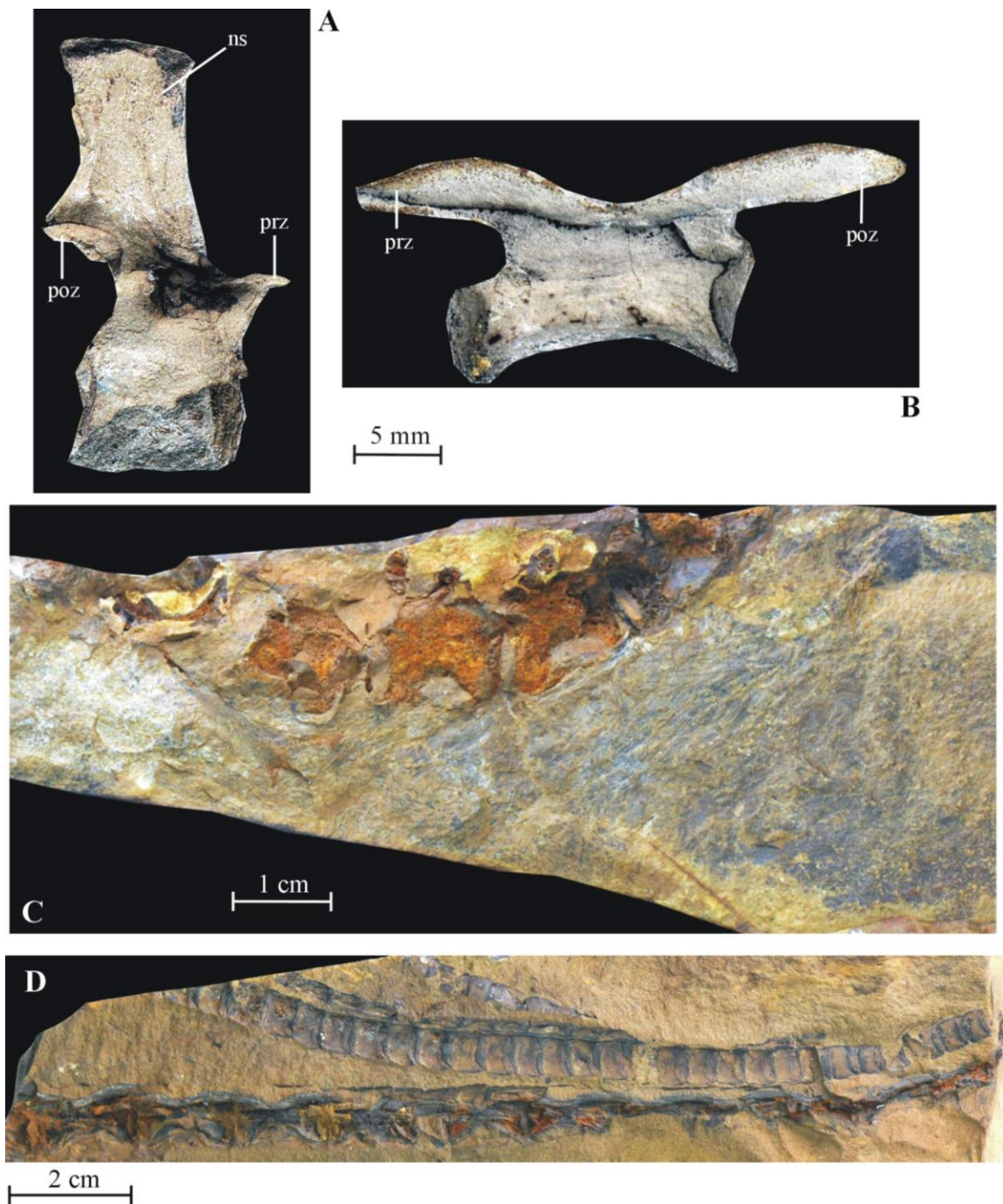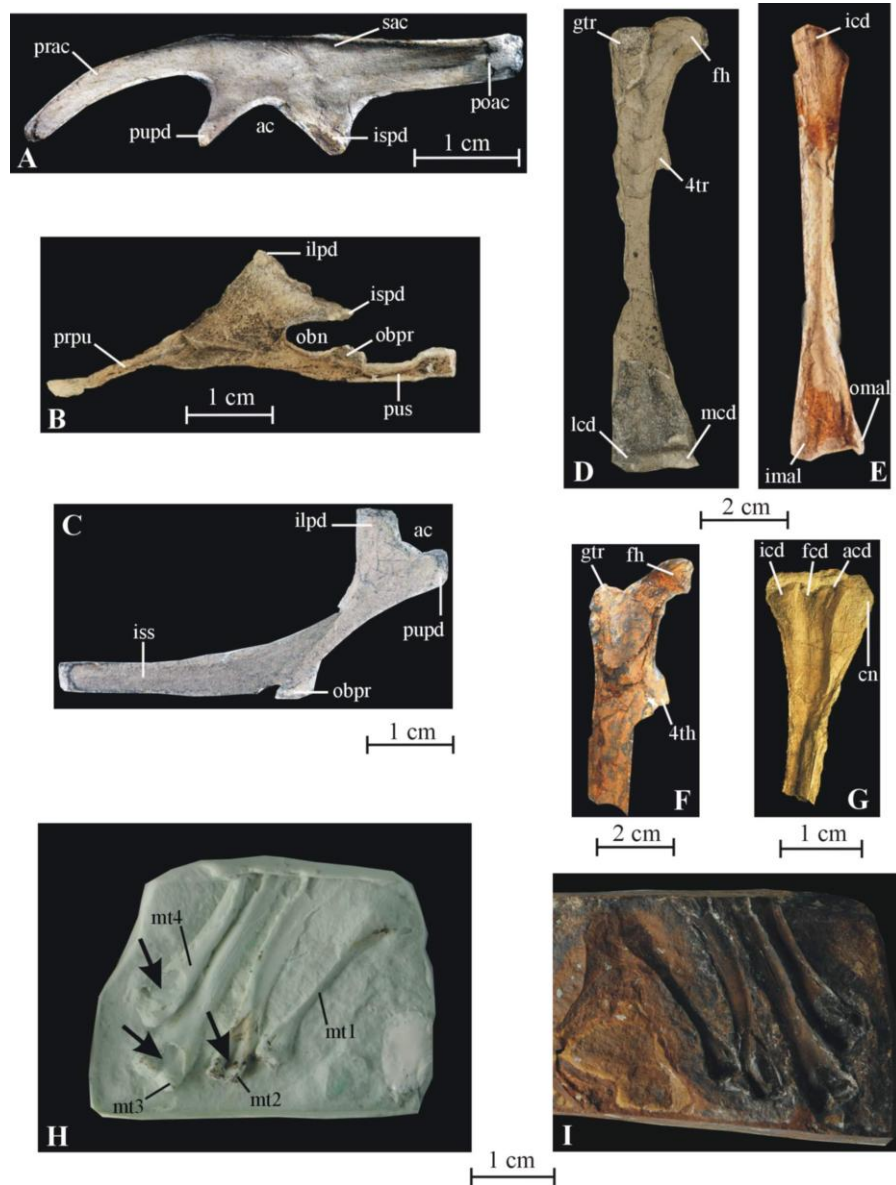
Fig. S5. *Kulindadromeus zabaikalicus* **nov. gen., nov. sp., from the Ukurey Fm (Middle to Late Jurassic) of Kulinda (Chitinskaya Oblast, Russia).** A, dorsal vertebra (INREC 3/112) in right lateral view; B, distal caudal vertebra(INREC K3/202) in left lateral view; C, proximal caudal vertebrae (INREC K4/150 in right lateral view; D, distal caudal vertebrae (INREC K4/159) in left lateral view, note the presence of imbricated scales (right row in ventral view) dorsal to the caudal vertebrae. Abbreviations: poz, postzygapophysis; prz, prezygapophysis.

Fig. S6. *Kulindadromeus zabaikalicus* **nov. gen., nov. sp., from the Ukurey Fm (Middle to Late Jurassic) of Kulinda (Chitinskaya Oblast, Russia).** A, Associated left humerus (top left, in caudal view) and scapula (bottom right, in lateral view) INREC K3/203; B, proximal portion of right scapula (INREC 204) in lateral view; C, left ulna (INREC K3/205) in medial view. Abbreviations: acp, acromial process; corf, coracoid facet; dpc, deltopectoral crest; drf, distal radial facet; gl, glenoid; hh, humeral head; hum, humerus; ol, olecranon process; prf, proximal radial facet; rcd, radial condyle; sc, scapula; ucd, ulnar condyle.
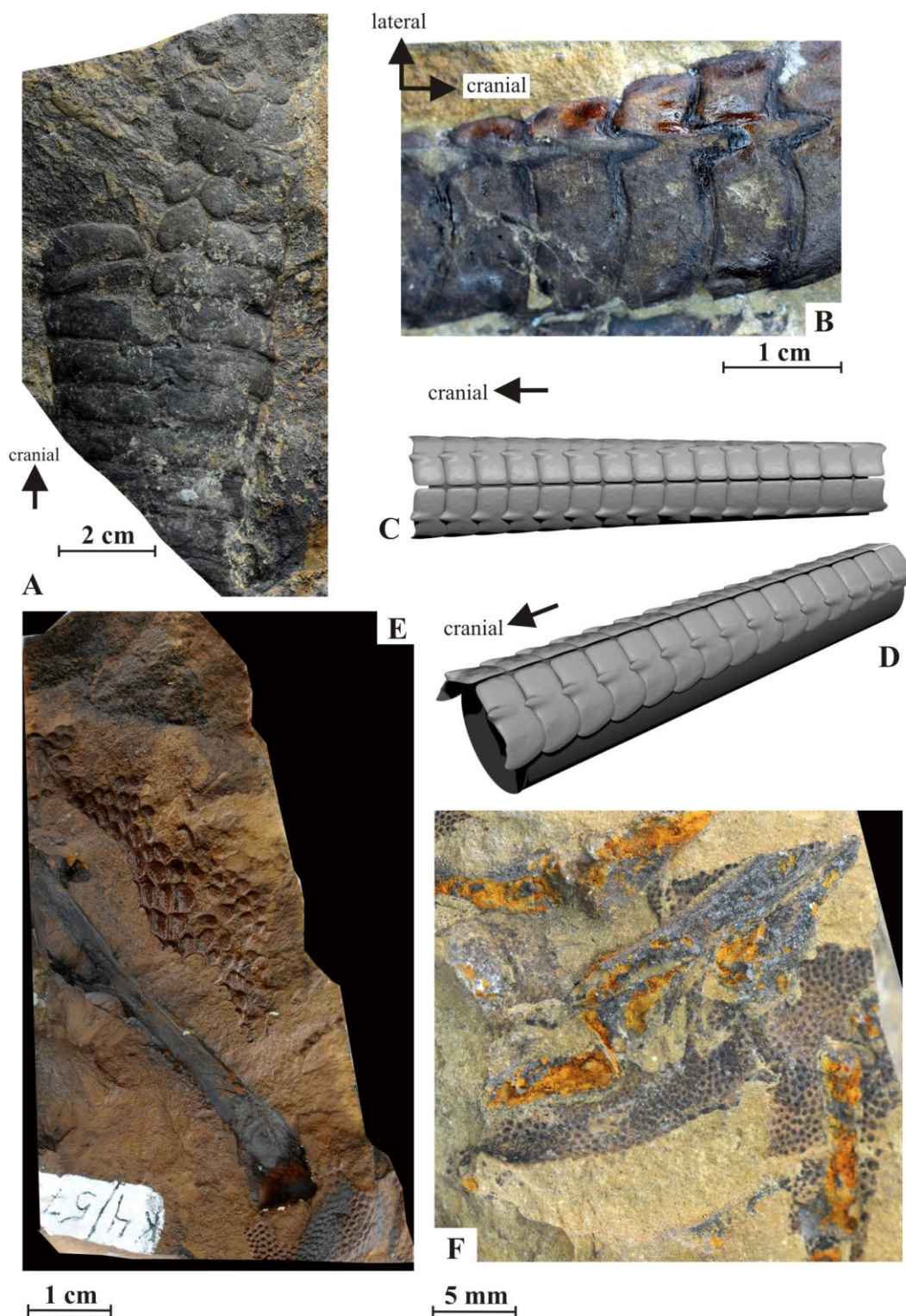
Fig. S7. *Kulindadromeus zabaikalicus* **nov. gen., nov. sp., from the Ukurey Fm (Middle to Late Jurassic) of Kulinda (Chitinskaya Oblast, Russia).** A, left ilium (INREC K3/113) in lateral view; B, left pubis (INREC K3/114) in lateral view; C, right ischium (INREC K3/124) in lateral view; D, right femur (INREC K3/206) in cranial view; E, right tibia (INREC K3/207) in caudal view; F, proximal part of right femur (INREC K3/208) in cranial view; G, proximal part of right tibia (INREC K3/209) in lateral view; H, mold of right metatarsus (INREC K4/72) in dorsal view, arrows indicate extensor fossa on distal end of metatarsals; I, right metatarsus (INREC K4/72) in dorsal view. Abbreviations: ac, actetabulum; acd, accessory condyle; cn, cnemial crest; fcd, fibular condyle; fh, femoral head; gtr, greater trochanter; icd, inner condyle; ilpd, iliac peduncle; imal, inner malleolus; ispd, ischiac peduncle; iss, ischial shaft; lcd, lateral condyle; mcd, medial condyle; mt, metatarsal; obn, obturator notch; obpr, obturator process; omal, outer malleolus; poac, postacetabular process; prac, preacetabular process; prpu, prepubic process; pupd, pubic peduncle; pus, pubic shaft; sac, supraacetabular crest; 4tr, fourth trochanter.
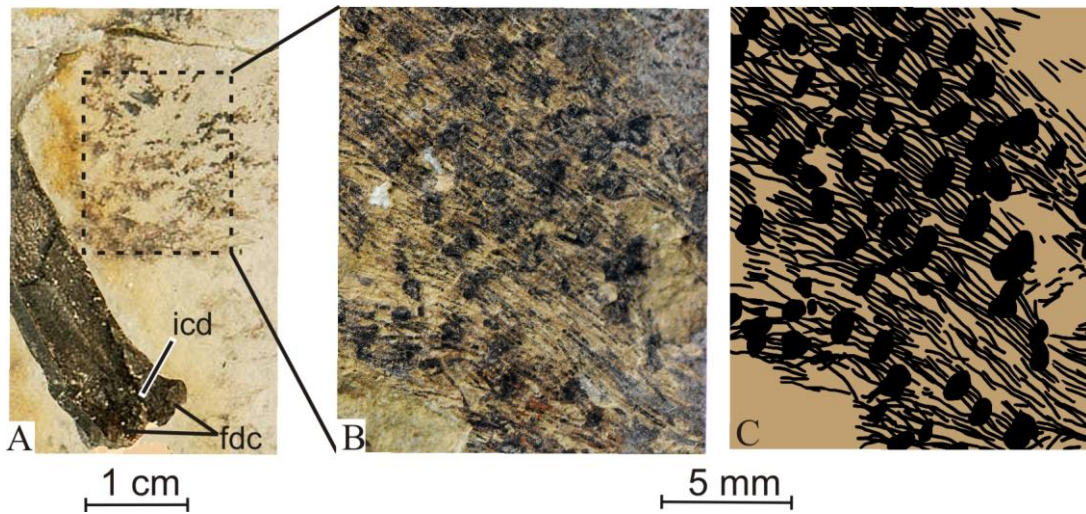
Fig. S8. Scales in *Kulindadromeus zabaikalicus* nov. gen., nov. sp., from the Ukurey Fm (Middle to Late Jurassic) of Kulinda (Chitinskaya Oblast, Russia). A, double row of scales above the proximal part of the tail (INREC K4/94) in dorsal view; B, close-up of the left row of caudal scales (INREC K4/117) in dorsal view; partial reconstruction of the caudal scales in dorsal (C) and laterodorsal (D) views; E, scales around the tibia and around the tarsus (INREC K4/57); F, scales around the right metatarsus and pes (INREC K4/118).

Fig. S9. Feather-like structures in *Kulindadromeus zabaikalicus* nov. gen., nov. sp., from the Ukurey Fm (Middle to Late Jurassic) of Kulinda (Chitinskaya Oblast, Russia). A, distal portion of left (?) femur (INREC K4/116) in caudal view; B, detail of compound structures around femur (counterpart of INREC K4/116); C, interpretative drawing of B, the black "blotches" represent the basal plates of the compound structures.
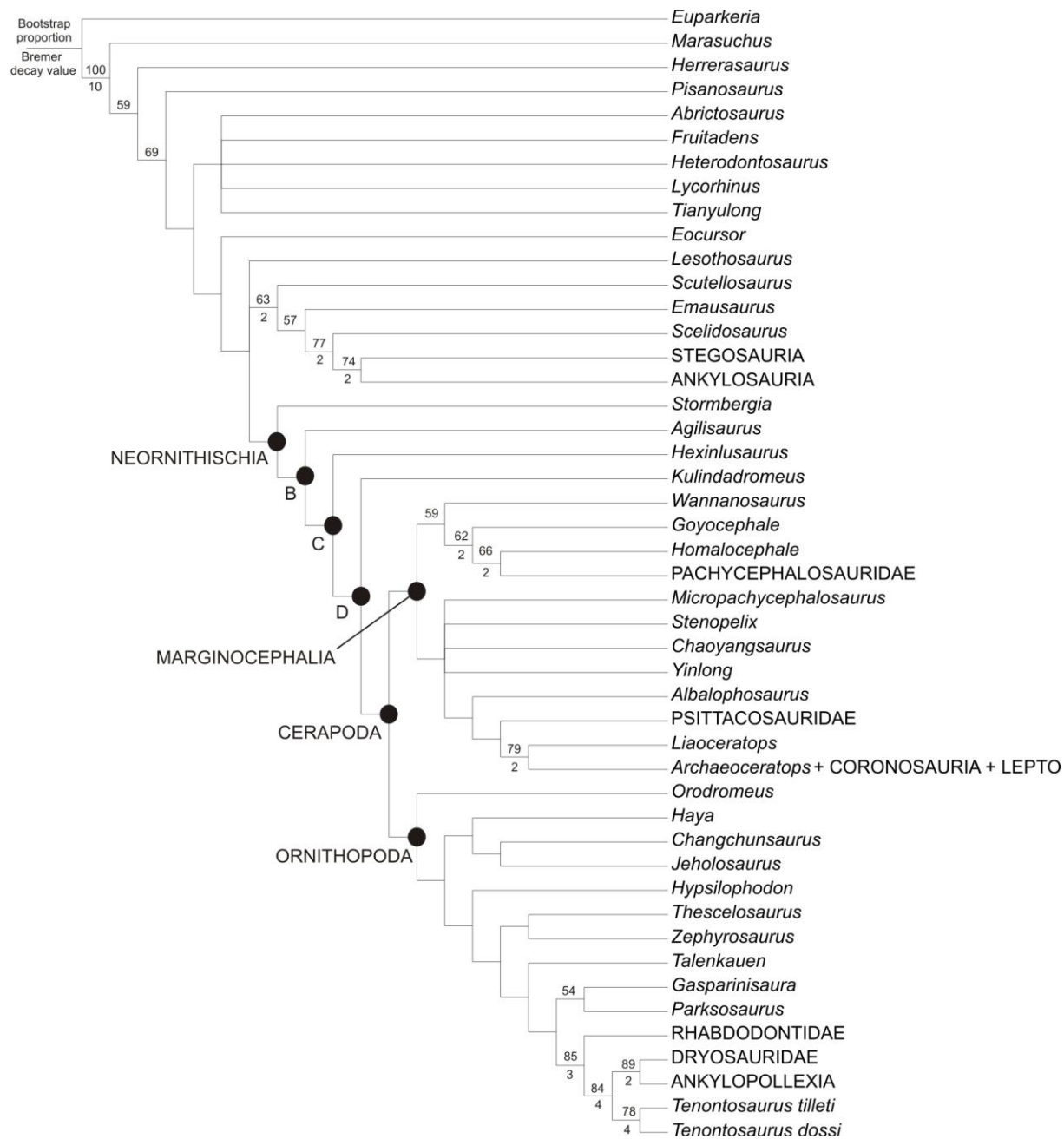
Fig. S10. Position of *Kulindadromeus zabaikalicus* within Ornithischia. The cladistic analysis is based on inclusion of *Kulindadromeus* in a recently published analysis of ornithischian phylogeny (Han et al., 2012). Strict consensus tree of 4 MPT's. Tree Length = 571; consistency index (CI) excluding uninformative characters = 0.42; Retention index (RI) = 0.7. Nodal support (Bremer indices) is indicated above each branch. The number below each branch refers to the different clades of the phylogeny. Bootstrap proportions lower than 50 and Bremer decay values lower than 2 are not indicated.
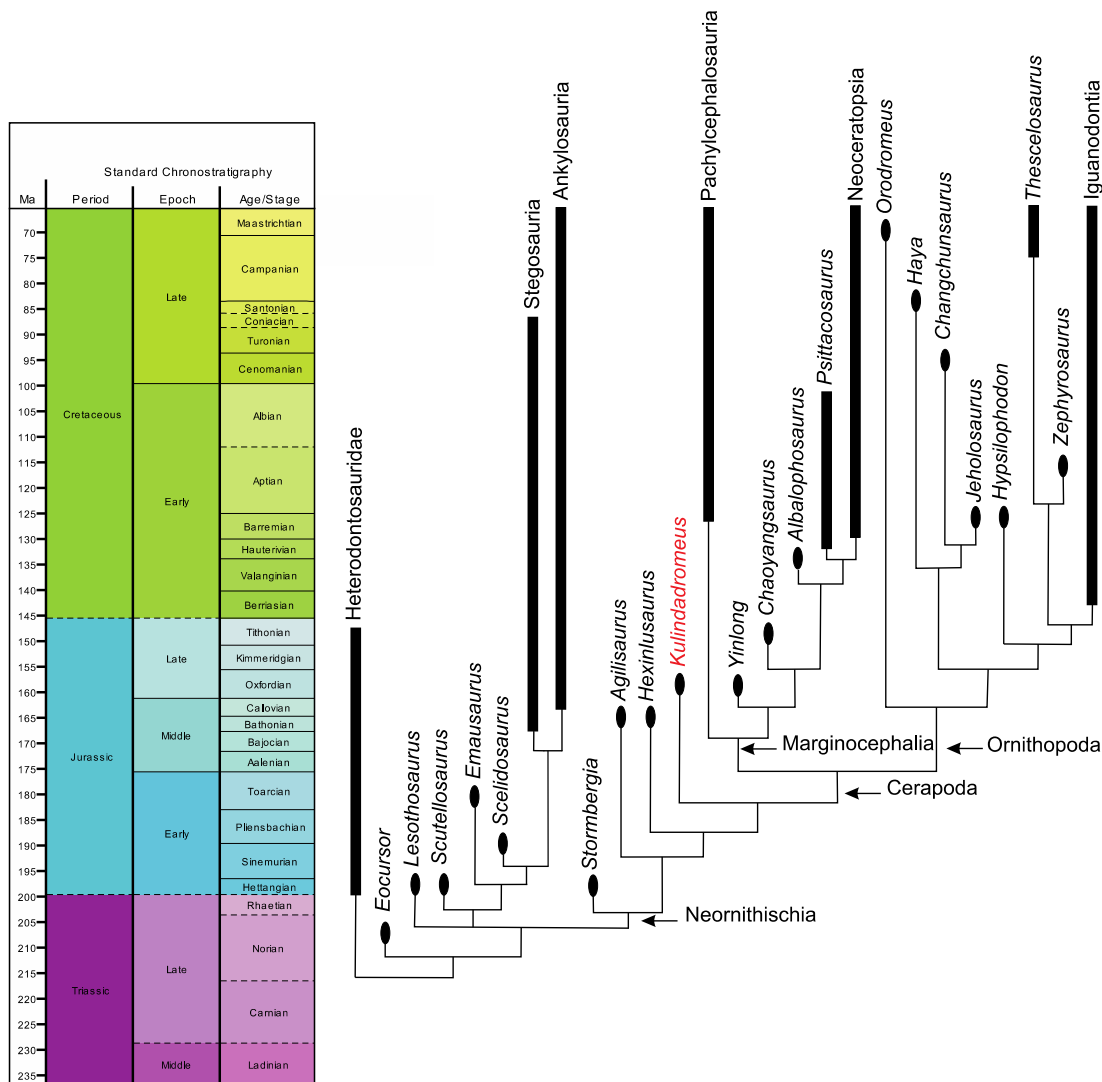
Fig. S11. Phylogenetic relationships of *Kulindadromeus zabaikalicus* among ornithischian dinosaurs, as a result of the inclusion of *Kulindadromeus* in a recently published analysis of ornithischian phylogeny. Time-calibrated strict consensus tree of the 4 most parsimonious trees (tree length = 571; consistency index excluding uninformative characters = 0.42; retention index = 0.7). In this hypothesis, *Kulindadromeus* is the sister-taxon of Cerapoda.

References and Notes

1. M. A. Norell, X. Xu, Feathered dinosaurs. *Annu. Rev. Earth Planet. Sci.* **33**, 277–299 (2005). doi:10.1146/annurev.earth.33.092203.122511

2. T. Lingham Solia, A. Feduccia, X. Wang, *Proc. Biol. Sci.* **274**, 2823 (2007).

3. F. Zhang, Z. Zhou, G. Dyke, Feathers and 'feather-like' integumentary structures in Liaoning birds and dinosaurs. *Geol. J.* **41**, 395 (2006). doi:10.1002/gj.1057

4. T. Lingham-Soliar, A unique cross section through the skin of the dinosaur *Psittacosaurus* from China showing a complex fibre architecture. *Proc. Biol. Sci.* **275**, 775–780 (2008). Medline doi:10.1098/rspb.2007.1342

5. D. Hu, L. Hou, L. Zhang, X. Xu, A pre-*Archaeopteryx* troodontid theropod from China with long feathers on the metatarsus. *Nature* **461**, 640–643 (2009). Medline doi:10.1038/nature08322

6. S. L. Brusatte, S. J. Nesbitt, R. B. Irmis, R. J. Butler, M. J. Benton, M. A. Norell, The origin and early radiation of dinosaurs. *Earth Sci. Rev.* **101**, 68–100 (2010). doi:10.1016/j.earscirev.2010.04.001

7. X. Xu, H. You, K. Du, F. Han, An *Archaeopteryx*-like theropod from China and the origin of Avialae. *Nature* **475**, 465–470 (2011). Medline doi:10.1038/nature10288

8. P. Godefroit, H. Demuynck, G. Dyke, D. Hu, F. Escuillié, P. Claeys, Reduced plumage and flight ability of a new Jurassic paravian theropod from China. *Nat. Commun.* **4**, 1394 (2013). Medline doi:10.1038/ncomms2389

9. P. Godefroit, A. Cau, H. Dong-Yu, F. Escuillié, W. Wenhao, G. Dyke, A Jurassic avialan dinosaur from China resolves the early phylogenetic history of birds. *Nature* **498**, 359–362 (2013). Medline doi:10.1038/nature12168

10. F. Zhang, S. L. Kearns, P. J. Orr, M. J. Benton, Z. Zhou, D. Johnson, X. Xu, X. Wang, Fossilized melanosomes and the colour of Cretaceous dinosaurs and birds. *Nature* **463**, 1075–1078 (2010). Medline doi:10.1038/nature08740

11. Q. Li, K. Q. Gao, J. Vinther, M. D. Shawkey, J. A. Clarke, L. D'Alba, Q. Meng, D. E. Briggs, R. O. Prum, Plumage color patterns of an extinct dinosaur. *Science* **327**, 1369–1372 (2010). Medline doi:10.1126/science.1186290

12. G. Mayr, D. S. Peters, G. Plodowski, O. Vogel, Bristle-like integumentary structures at the tail of the horned dinosaur *Psittacosaurus*. *Naturwissenschaften* **89**, 361–365 (2002). Medline doi:10.1007/s00114-002-0339-6

13. X.-T. Zheng, H.-L. You, X. Xu, Z.-M. Dong, An Early Cretaceous heterodontosaurid dinosaur with filamentous integumentary structures. *Nature* **458**, 333–336 (2009). Medline doi:10.1038/nature07856

14. O. W. M. Rauhut, C. Foth, H. Tischlinger, M. A. Norell, Exceptionally preserved juvenile megalosauroid theropod dinosaur with filamentous integument from the Late Jurassic of Germany. *Proc. Natl. Acad. Sci. U.S.A.* **109**, 11746–11751 (2012). Medline doi:10.1073/pnas.1203238109

15. See the supplementary materials on *Science* Online.

16. R. J. Butler, P. Upchurch, D. B. Norman, The phylogeny of the ornithischian dinosaurs. *J. Syst. Palaeontology* **6**, 1–40 (2008). doi:10.1017/S1477201907002271

17. A. M. Lucas, P. R. Stettenheim, *Avian Anatomy, Integument* (U.S. Department of Agriculture, Washington, DC, 1972).

18. M. K. Vickarious, T. Maryanska, D. B. Weishampel, in *The Dinosauria 2nd edn*, D. B. Weishampel, P. Dodson, H. Osmolska, Eds. (Univ. of California Press, Berkeley, CA, 2004), pp. 363–392.

19. P. R. Bell, Standardized terminology and potential taxonomic utility for hadrosaurid skin impressions: A case study for *Saurolophus* from Canada and Mongolia. *PLOS ONE* **7**, e31295 (2012). Medline doi:10.1371/journal.pone.0031295

20. P. J. Currie, P. J. Chen, Anatomy of *Sinosauropteryx prima* from Liaoning, northeastern China. *Can. J. Earth Sci.* **38**, 1705–1727 (2001). doi:10.1139/e01-050

21. X. Xu, X. Zheng, H. You, Exceptional dinosaur fossils show ontogenetic development of early feathers. *Nature* **464**, 1338–1341 (2010). Medline doi:10.1038/nature08965

22. F. Zhang, Z. Zhou, X. Xu, X. Wang, C. Sullivan, A bizarre Jurassic maniraptoran from China with elongate ribbon-like feathers. *Nature* **455**, 1105–1108 (2008). Medline doi:10.1038/nature07447

23. M. Buchwitz, S.Voigt, *Paläontol. Z.* **86**, 313 (2012).

24. X. Wang, Z. Zhou, F. Zhang, X. Xu, A nearly completely articulated rhamphorhynchoid pterosaur with exceptionally well-preserved wing membranes and? hairs? from Inner Mongolia, northeast China. *Chin. Sci. Bull.* **47**, 226 (2002). doi:10.1360/02tb9054

25. X. Zheng, Z. Zhou, X. Wang, F. Zhang, X. Zhang, Y. Wang, G. Wei, S. Wang, X. Xu, Hind wings in basal birds and the evolution of leg feathers. *Science* **339**, 1309–1312 (2013). Medline doi:10.1126/science.1228753

26. D. Dhouailly, A new scenario for the evolutionary origin of hair, feather, and avian scales. *J. Anat.* **214**, 587–606 (2009). Medline doi:10.1111/j.1469-7580.2008.01041.x

27. F. Prin, D. Dhouailly, How and when the regional competence of chick epidermis is established: Feathers vs. scutate and reticulate scales, a problem en route to a solution. *Int. J. Dev. Biol.* **48**, 137–148 (2004). Medline doi:10.1387/ijdb.15272378

28. N. Shubin, C. Tabin, S. Carroll, Fossils, genes and the evolution of animal limbs. *Nature* **388**, 639–648 (1997). Medline doi:10.1038/41710

29. S. M. Sinitsa, in *Environmental Cooperative Studies in the Cross-Border Ecological Region: Russia, China, and Mongolia*, S. M. Sinitsa, Ed. (Institute of Natural Resources, Ecology and Cryology, Siberian Branch of the Russian Academy of Sciences, Chita, Russia, 2011), pp. 173–176.

30. S. M. Sinitsa, S. Starukhina, in *Novye dannye po geologii Zabaikal'ya* (Ministry of Geology, Russian Soviet Federative Socialist Republic, Moscow, 1986), pp. 46–51.

31. F. M. Gradstein *et al.*, *The Geologic Time Scale 2012* (Elsevier, Boston, 2012).

32. R. L. Lyman, *Vertebrate Taphonomy* (Cambridge Univ. Press, Cambridge, 1994).

33. P. M. Barrett, F.-H. Han, *Zootaxa* **2072**, 31 (2009).

34. P. C. Sereno, Taxonomy, morphology, masticatory function and phylogeny of heterodontosaurid dinosaurs. *ZooKeys* **226**, 1–225 (2012). Medline doi:10.3897/zookeys.226.2840

35. F. Knoll, Nearly complete skull of *Lesothosaurus* (Dinosauria: Ornithischia) from the Upper Elliot Formation (Lower Jurassic: Hettangian) of Lesotho. *J. Vertebr. Paleontol.* **22**, 238–243 (2002). doi:10.1671/0272-4634(2002)022[0238:NCSOLD]2.0.CO;2

36. P. M. Galton, *Bull. British Mus. Nat. Hist. Geol.* **25**, 1 (1974).

37. P. J. Makovicky, B. M. Kilbourne, R. W. Sadleir, M. A. Norell, A new basal ornithopod (Dinosauria, Ornithischia) from the Late Cretaceous of Mongolia. *J. Vertebr. Paleontol.* **31**, 626–640 (2011). doi:10.1080/02724634.2011.557114

38. P. M. Barrett, R. J. Butler, F. Knoll, Small-bodied ornithischian dinosaurs from the Middle Jurassic of Sichuan, China. *J. Vertebr. Paleontol.* **25**, 823–834 (2005). doi:10.1671/0272-4634(2005)025[0823:SODFTM]2.0.CO;2

39. L. Jin, J. Chen, S. Zan, R. J. Butler, P. Godefroit, The first *Dictyoolithus* egg clutches from the Lishui Basin, Zhejiang Province, China. *J. Vertebr. Paleontol.* **30**, 196–214 (2010).

40. R. D. Scheetz, thesis, Montana State University, Bozeman, MT 1999).

41. P. C. Sereno, thesis, Columbia University, New York 1986).

42. D. B. Norman, H.-D. Sues, L. M. Witmer, R. Coria, in *The Dinosauria 2nd edn*, D. B. Weishampel, P. Dodson, H. Osmolska, Eds. (Univ. of California Press, Berkeley, CA, 2004), pp. 393–412.

43. H.-D. Sues, *Palaeontographica A* **169**, 51 (1980).

44. D. B. Norman, L. M. Witmer, D. B. Weishampel, in *The Dinosauria 2nd edn*, D. B. Weishampel, P. Dodson, H. Osmolska, Eds. (Univ. of California Press, Berkeley, CA, 2004), pp. 325–334.

45. P. M. Galton, *Revue Paléobiol.* **16**, 231 (1997).

46. P. M. Galton, *Revue Paléobiol.* **18**, 517 (1997).

47. M. Huh, D.-G. Lee, J.-K. Kim, J.-D. Lim, P. Godefroit, A new basal ornithopod dinosaur from the Upper Cretaceous of South Korea. *Neues Jahrb. Geol. Palaontol. Abh.* **259**, 1–24 (2011). doi:10.1127/0077-7749/2010/0102

48. R. J. Butler, L.-Y. Jin, J. Chen, P. Godefroit, *Palaeontology* **5**, 667 (2010).

49. D. J. Varricchio, A. J. Martin, Y. Katsura, First trace and body fossil evidence of a burrowing, denning dinosaur. *Proc. Biol. Sci.* **274**, 1361–1368 (2007). Medline doi:10.1098/rspb.2006.0443

50. F.-L. Han, P. M. Barrett, R. J. Butler, X. Xu, Postcranial anatomy of *Jeholosaurus shangyuanensis* (Dinosauria, Ornithischia) from the Lower Cretaceous Yixian Formation of China. *J. Vertebr. Paleontol.* **32**, 1370–1395 (2012). doi:10.1080/02724634.2012.694385

51. T. Lingham-Soliar, Dinosaur protofeathers: Pushing back the origin of feathers into the Middle Triassic? *J. Ornithol.* **151**, 193–200 (2010). doi:10.1007/s10336-009-0446-7

52. R. O. Prum, Development and evolutionary origin of feathers. *J. Exp. Zool.* **285**, 291–306 (1999). Medline doi:10.1002/(SICI)1097-010X(19991215)285:4<291::AID-JEZ1>3.0.CO;2-9

53. R. O. Prum, A. H. Brush, The evolutionary origin and diversification of feathers. *Q. Rev. Biol.* **77**, 261–295 (2002). Medline doi:10.1086/341993

54. P. A. Goloboff, J. Farris, K. C. Nixon, TNT, a free program for phylogenetic analysis. *Cladistics* **24**, 774–786 (2008). doi:10.1111/j.1096-0031.2008.00217.x

55. K. C. Nixon, *WinClada ver. 1.00.08* (published by the author, Ithaca, NY, 2004).